

Absorption contribution to the pion double-charge-exchange reaction

E. Oset,* M. Khankhasayev,[†] J. Nieves,* H. Sarafian,[‡] and M. J. Vicente-Vacas*

Institute for Nuclear Theory, University of Washington, Seattle, Washington 98195

(Received 16 March 1992)

We have evaluated the mechanism analogous to pion absorption which contributes to the pion double-charge-exchange amplitude leading to double isobar analog states. We find appreciable corrections at low energies around $T_\pi = 50$ MeV. Around the resonance region the corrections are small and the most visible effect is a small shift of the minimum to smaller angles, which is however not big enough to reproduce the experimental data.

PACS number(s): 25.80.Gn

I. INTRODUCTION

The pion-nucleus double-charge-exchange (DCX) reaction has attracted much attention during the last years [1,2]. Both at low energies and in the resonance region, there are several striking features which are not yet understood. At low energies the angular distributions are forward peaked and the forward-angle cross section are large [3], in contrast with the deep forward-angle minimum in the cross section for single charge exchange [4]. In the resonance region, the position of the first minimum occurs at an angle of about 20° , substantially lower than typical diffraction-model estimates [5].

The results of many microscopic calculations [2,6–9] show that the sequential (SEQ) mechanism does not describe these features of the DCX reaction. Meson-exchange currents have also been investigated [6,10,11] and have been found to be small in double isobar analog (DIAS) transitions around resonance, and in any case they do not produce a shift in the minimum. One DCX mechanism associated with pion absorption has been suggested a few times as a candidate to solve the puzzle [6,9,12].

The present paper is aimed at considering the role of this absorption mechanism for the DIAS transitions, both at low energy and at the resonance regions. There are several arguments in favor of the importance of this absorption channel in DCX. First, it is known that pion absorption has a strong effect on elastic scattering both at low energies [13–16] and at resonance [17]. Second, it is also known that a fraction of pions is absorbed by two nucleons of total isospin 1 (see, e.g., [18]; DCX converts a pair of neutrons to a pair of protons or vice versa). Third, it has been argued that the absorption mechanism might be responsible for the shift of the first minimum in

the differential cross section to smaller angles at resonance energies [6,9]. In this paper we evaluate this piece of the DCX amplitude consistently with present knowledge of the pion-absorption problem and study its repercussion on the DCX cross sections.

II. ABSORPTION CONTRIBUTION TO DCX AT RESONANCE

One of the puzzling and unexplained features of DCX is the position of the first minimum in the differential cross section of (π^+, π^-) in ^{18}O at $T_\pi = 164$ MeV [3,5]. Phenomenological analyses point to the need for an additional mechanism. The interference of the amplitude of this complementary mechanism with the standard sequential single charge exchange is expected to provide an acceptable solution [19,20]. Unconventional mechanisms such as exchange currents related to the pion pole or contact terms in $\pi N \rightarrow 2\pi N$ were investigated in [10] and did not lead to appreciable changes in the position of the minimum. Furthermore, a new reformulation of these exchange currents with the different variants of the chiral Lagrangians is done in [11]. Another sort of exchange current related to the Δ interaction in the medium (DINT mechanism) [21] was also found to be unable to produce shifts in the minimum [6].

The reason for these failures is to be found in the fact that around the resonance region the conventional mechanism depicted in Fig. 1(a) has an amplitude which is purely imaginary (when the deltas and the intermediate pion are placed on shell), while the amplitude for the mechanisms depicted in Fig. 1(b) and 1(c) is purely real. Hence there is no interference between these amplitudes, and consequently the minimum is barely shifted. It is thus clear that the chances for a shift would be far better if one had a mechanism which also produced an imaginary amplitude around resonance or a complex one with a sizable imaginary part. One such mechanism, the absorption contribution to DCX which we depict in Fig. 2(a), has been suggested before [6,9,12]. However, no actual calculation was ever performed for such pieces. We evaluate it in this section. In doing so, our guiding principle has been to use the same model which was used to evaluate the Δ self-energy in [22], since consistency of the

*Permanent address: Departamento de Física Teórica and IFIC, Centro Mixto Universidad de Valencia-CSIC, 46100 Burjassot, Valencia, Spain.

[†]Permanent address: Joint Institute for Nuclear Research, Laboratory of Theoretical Physics, 141980 Dubna, Russia.

[‡]Permanent address: Department of Physics, Pennsylvania State University, York, PA 17403.

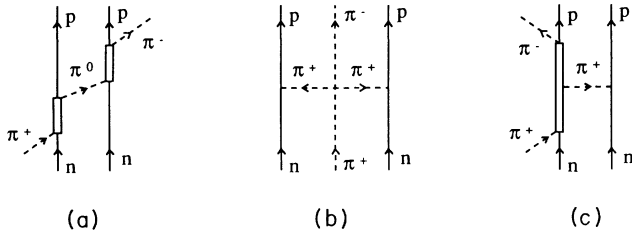


FIG. 1. Feynman diagrams with different mechanisms contributing to DCX: (a) conventional or sequential DCX, (b) meson-exchange current contribution to DCX from the pion pole term, and (c) delta interaction mechanism to DCX.

results with the empirical information of [23] was reached, and furthermore the approach leads to a fair reproduction of the pion nucleus elastic [17] and reaction cross sections [24], including absorption and related reactions such as (π^+, pp) and (π^-, pp) [32] which test the isospin dependence of the model. Indeed, if instead of having charge exchange we had a $\pi^+ NN \rightarrow \pi^+ NN$ process (in Fig. 2) and we summed over the occupied states for the nucleon lines, we would get the diagram of Fig. 2(b), which is a pion self-energy diagram coming from Δh excitation with the Δ self-energy incorporated. It is thus clear that apart from the sums over the occupied states in Fig. 2(b) the only difference between Figs. 2(a) and 2(b) comes from the isospin dependence of the diagrams, which is rather easy to work out. Figure 2(a) is called the “absorption” mechanism contributing to DCX because the dissociated upper and/or lower half of the diagram cut by the dotted line represents pion absorption in the equivalent process of pion scattering depicted in Fig. 2(b). When in the intermediate integrations the particles cut by a line are placed on shell, one obtains an imaginary

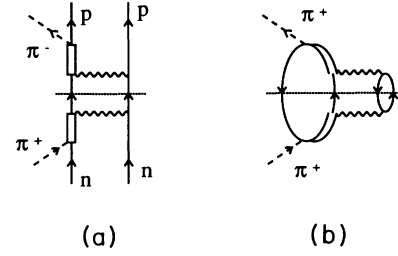


FIG. 2. (a) Feynman diagram representing the absorption contribution to DCX and (b) corresponding diagram accounting for two-body pion absorption in the pion nucleus optical potential.

contribution to the amplitude. Hence the absorption cut in Fig. 2(a) leads to an imaginary piece which can interfere with the conventional mechanism of Fig. 1(a).

The first thing to realize is that in Fig. 2(a) or 2(b) the interaction lines are largely dominated by the transverse part of the spin-isospin effective interaction [22], which is essentially given by the g' Landau parameter. What we want to stress with that point is the fact that this interaction is roughly constant in momentum space and hence corresponds to a very-short-range effective interaction in coordinate space. In studies of nuclear excitations with electromagnetic probes, it is indeed simulated by a $\delta(\mathbf{r})$ function [25]. We will use this fact, which allows us to approximate the contribution of Fig. 2(a) by assuming equal coordinates in the two baryonic lines of Fig. 2(a). In addition, we shall apply the ordinary closure sum over the nucleon and delta states, as is usually done in studies of DCX [6,21]. Therefore, to a good approximation, this leaves us only one spatial coordinate.

The S matrix of the process of Fig. 2(a), in Mandl-Shaw notation [26], is then given by

$$S = 1 - i \frac{1}{V} \frac{1}{\sqrt{2\omega(k)}} \frac{1}{\sqrt{2\omega(k')}} 2\pi \delta(E_i - E_f) \int d^3\mathbf{x} \phi_i^*(\mathbf{x}) \phi_j^*(\mathbf{x}) e^{i(\mathbf{k}-\mathbf{k}')\cdot\mathbf{x}} T \phi_i(\mathbf{x}) \phi_j(\mathbf{x}), \quad (1)$$

where the variables are shown explicitly in Fig. 3. V is the volume of the box where the pions are confined, and ϕ is the wave function of the nucleons. E_i, E_f stand for the energy of the initial and final states, and T is the T matrix of the process which will depend on the pion momenta \mathbf{k}, \mathbf{k}' and the spin and isospin of the particles.

Now assume we would like to calculate the self-energy of the pion in nuclear matter starting with the diagram of Fig. 3, with π^- colliding against two protons. This is depicted in Fig. 4(a), and it leads to the pion self-energy piece of Fig. 4(b). The π self-energy in nuclear matter would thus be calculated, neglecting Pauli blocking on the particle lines, as

$$\begin{aligned} -i\Pi^{(p,p)}(k) &= \sum_{s_1} \int \frac{d^3\mathbf{p}_1}{(2\pi)^3} n(\mathbf{p}_1) \sum_{s_2} \int \frac{d^3\mathbf{p}_2}{(2\pi)^3} n(\mathbf{p}_2) (-i) T_{s_1, s_2, s_1, s_2} \\ &= -i\bar{T} \rho_p \rho_p, \end{aligned} \quad (2)$$

with ρ_p the proton density and \bar{T} the average over spins and momenta of the spin diagonal T matrix. Since the two nucleon mechanisms are usually dominated by the diagonal spin transitions [6,10], it is a proper approximation to replace T in Eq. (1) by its spin average of Eq. (2). Hence the T matrix for the open diagram (Fig. 3), with $\pi^- pp \rightarrow \pi^- pp$, is then given by

$$t = \int d^3\mathbf{x} \phi_i^*(\mathbf{x}) \phi_j^*(\mathbf{x}) e^{i(\mathbf{k}-\mathbf{k}')\cdot\mathbf{x}} \frac{\Pi^{(p,p)}}{\rho_p^2} \phi_i(\mathbf{x}) \phi_j(\mathbf{x}). \quad (3)$$

Equation (3) has the virtue of allowing us to determine the amplitude for the open diagram in terms of the pion self-energy, which has already been evaluated and contrasted with different pion nuclear experiments.

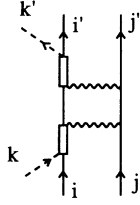


FIG. 3. Same as diagram of Fig. 2(a) with labels for the particle states.

There are still two points to be considered. One is a transition from $\Pi^{(p,p)}$ in nuclear matter to finite nuclei, and the other one is to construct the t matrix for $\pi^+ nn \rightarrow \pi^- pp$, which is the one we are concerned about.

Let us recall that the pion self-energy associated with the diagram of Fig. 4(b) is given by [17]

$$\Pi(k) = \frac{4}{9} \left(\frac{f^*}{\mu} \right)^2 \rho k^2 \frac{M^2}{\bar{s}} \frac{\Sigma_\Delta}{[\sqrt{\bar{s}} - M_\Delta + i(\bar{\Gamma}/2) - \Sigma_\Delta]^2}, \quad (4)$$

with Σ_Δ the Δ self-energy corresponding to the diagram in Fig. 4(b) when the hole line and external pion lines are removed. In the formula, \bar{s} is the average value of the Mandelstam variable for the incoming πN system forming the delta and $\bar{\Gamma}$ the Pauli-corrected Δ width given by

$$\begin{aligned} \frac{\bar{\Gamma}}{2} = & \frac{1}{3} \frac{1}{4\pi} \frac{f^{*2}}{\mu^2} q_N^3 \frac{M}{\sqrt{\bar{s}}} \\ & \times \left[1 + \theta(q_N - k_F) \left(-\frac{1}{5} \frac{k_F^2}{q_N^2} \right) \right. \\ & \left. + \theta(k_F - q_N) \left(\frac{q_N}{k_F} - 1 - \frac{1}{5} \frac{q_N^3}{k_F^3} \right) \right], \quad (5) \end{aligned}$$

where q_N is the c.m. momentum of the nucleon (or pion) for the decay of a Δ of mass $\sqrt{\bar{s}}$, μ is the pion mass, f^* is the $\pi N \Delta$ coupling constant ($f^{*2}/4\pi = 0.36$), and k_F is the Fermi momentum,

$$k_F = \left(\frac{3\pi^2}{2} \rho(\mathbf{r}) \right)^{1/3}. \quad (6)$$

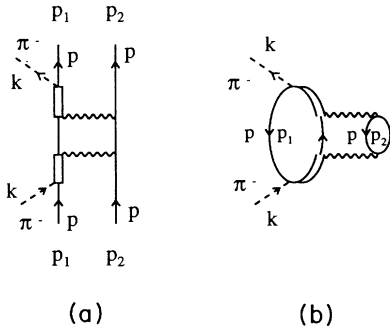


FIG. 4. (a) Feynman diagram for $\pi^- pp \rightarrow \pi^- pp$ through the absorption mechanism and (b) the sum over the external nucleon lines in (a), when they represent occupied states, leading to a π^- self-energy diagram.

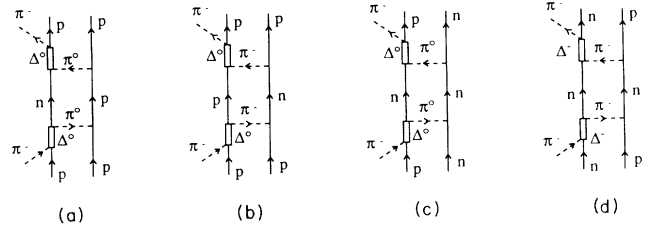


FIG. 5. Different isospin combinations in $\pi^- NN \rightarrow \pi^- NN$ through the absorption mechanisms.

In addition, Σ_Δ is roughly proportional to ρ , and hence

$$\Sigma_\Delta = \hat{\Sigma}_\Delta \rho / \rho_0. \quad (7)$$

Hence we obtain $\Pi(k)$ proportional to ρ^2 . Of course, this contains ρ_p^2 and $\rho_p \rho_n$ for a π^- (there is no absorption of a π^- by nn pairs). The separation is trivial and involves only manipulating Clebsch-Gordan coefficients. We shall work it out in detail for the Δ case, and this will illustrate how it is done for the other diagrams which enter in the low-energy region. The separation into ρ_p^2 and $\rho_p \rho_n$ is done in detail in [16] for low-energy pions, and we shall take the results from there. For the Δ case, we have the possible diagrams depicted in Fig. 5. The isospin coefficients are 1 (−1) for $\pi^0 pp$ (nn) coupling, $\sqrt{2}$ for a charged pion coupled to nucleons, and $C(1, 1/2, 3/2; t_\pi, t_N, t_\Delta)$ for the $\pi N \rightarrow \Delta$ vertex with a minus sign when there is an incoming π^+ ($|\pi^+\rangle = -|11\rangle$ in the Bjorken-Drell convention [27]). So we have, for the different terms,

$$C_a = \frac{2}{9}, \quad C_b = \frac{2}{9}, \quad C_c = \frac{2}{9}, \quad C_d = 2. \quad (8)$$

This means that the term $\frac{2}{3}\rho^2$ in Eq. (4) is actually

$$\frac{2}{3}\rho^2 \rightarrow \frac{4}{9}\rho_p^2 + \frac{20}{9}\rho_p \rho_n, \quad (9)$$

showing that absorption by np pairs dominates clearly as seen experimentally. From Fig. 6 for $\pi^+ nn \rightarrow \pi^- pp$ we get the coefficients

$$C_e = \frac{2}{9}, \quad C_f = \frac{2}{9}, \quad (10)$$

corresponding to Figs. 6(a) and 6(b), respectively. Hence the total isospin coefficient in $\pi^+ nn \rightarrow \pi^- pp$ is $\frac{4}{9}$, the same as in the $\pi^- pp \rightarrow \pi^- pp$ transition.

This little exercise serves us to write the DCX amplitude corresponding to Fig. 2(a) as

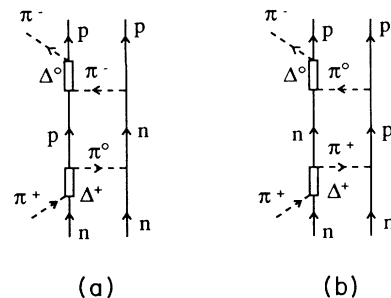


FIG. 6. Different isospin combinations in $\pi^+ nn \rightarrow \pi^- pp$.

$$t^{(\text{DCXA})}(k, k') = \frac{4}{3} \frac{4}{9} \left[\frac{f^*}{\mu} \right]^2 \mathbf{k} \cdot \mathbf{k}' \frac{M^2}{\bar{s}} \int d^3x \phi_i^*(\mathbf{x}) \phi_j^*(\mathbf{x}) e^{i(\mathbf{k}-\mathbf{k}') \cdot \mathbf{x}} \phi_i(\mathbf{x}) \phi_j(\mathbf{x}) \frac{\hat{\Sigma}_\Delta / \rho_0}{[\sqrt{\bar{s}} - M_\Delta + i(\bar{\Gamma}/2) - \Sigma_\Delta]^2}, \quad (11)$$

where we have implemented the trivial change $\mathbf{k}^2 \rightarrow \mathbf{k} \cdot \mathbf{k}'$, since the factor $\mathbf{k} \cdot \mathbf{k}'$ is the one actually appearing in finite nuclei, while in nuclear matter it is \mathbf{k}^2 , since in the latter case the pions propagate in the forward direction.

Equation (11) also incorporates already an extra factor of 2 to account for the possibility that the Δ excitation occurs in the second nucleon rather than the first one in the open diagrams [6,9]. This implies that antisymmetric wave functions for the initial and final two-body states, normalized to unity, must be used.

For $\hat{\Sigma}_\Delta$ around resonance, we have taken the results of [22]

$$\hat{\Sigma}_\Delta = \left[-33 - iC_{A2} \left(\frac{\rho}{\rho_0} \right)^{\beta-1} \right] \text{MeV} + \frac{4}{9} \left[\frac{f^*}{\mu} \right]^2 g'_{\Delta} \rho_0, \quad (12)$$

with $C_{A2} \approx 16.3$ MeV, $\beta \approx 0.8$ (actually, we have taken them as smooth functions of the pion kinetic energy [22]), and $g'_{\Delta} \approx 0.65$. We have added the last term in Eq. (12) in order to account for the coupling of the pion to Δh components which propagate iteratively [random-phase-approximation (RPA) sum] driven by the Landau-Migdal interaction [17].

The conventional mechanism, depicted in Fig. 7, is evaluated following [6] [Eq. (2.10)] after modifications to account for the Δ self-energy. Thus, ignoring the small spin-flip terms, we obtain

$$t^{(\text{DCX})}(\mathbf{k}, \mathbf{k}') = -\frac{4}{9} \left[\frac{f^*}{\mu} \right]^4 \int \frac{d^3p}{(2\pi)^3} \frac{2}{3} \mathbf{k} \cdot \mathbf{p} \frac{2}{3} \mathbf{k}' \cdot \mathbf{p} \frac{1}{p^{02} - \mathbf{p}^2 - \mu^2 + i\epsilon} \langle \phi_i | e^{i(\mathbf{k}-\mathbf{p}) \cdot \mathbf{x}} | \phi_i \rangle \times \left[\frac{1}{\sqrt{\bar{s}} - M_\Delta + \frac{1}{2}i\bar{\Gamma} - \Sigma_\Delta} \right]^2 \langle \phi_j | e^{i(\mathbf{p}-\mathbf{k}') \cdot \mathbf{x}} | \phi_j \rangle, \quad (13)$$

where the factor 2 of symmetry is already incorporated, and the cross section is given by

$$\frac{d\sigma}{d\Omega} = \left[\frac{1}{4\pi} \right]^2 |t^{(\text{DCXC})} + t^{(\text{DCXA})}|^2. \quad (14)$$

Since in the conventional mechanism the largest contribution comes from having the intermediate pion on shell [$-i\pi\delta(p^{02} - \mathbf{p}^2 - \mu^2)$ from the pion propagator], we can see that the imaginary part of the amplitude in the conventional mechanism is positive, while the one from the absorption mechanism is negative, and there is indeed an interference between the two amplitudes.

The distortion of the external and intermediate pions is very important at resonance, and we consider it in an eikonal form by following exactly the same procedure as in [6].

III. ABSORPTION CONTRIBUTION TO DCX AT LOW ENERGIES

We shall concentrate here on the region of $T_\pi = 50$ MeV where there have been experiments done. Our guiding principle here is to connect the DCX absorption amplitude with the absorption part of the optical potential.

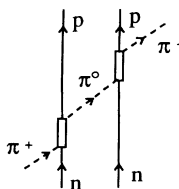


FIG. 7. Sequential DCX mechanism.

In [16] this latter problem was addressed and the potential led to a good reproduction of the absorption cross sections. The model for pion absorption consisted of the many-body diagrams shown in Fig. 8. It contains s -wave absorption [Fig. 8(a)] and p -wave absorption [Figs. 8(b) and 8(c)]. The s -wave absorption piece is worked out in detail in [28], while the p -wave absorption is done in [16].

For the p -wave πN amplitude, we use the model of Fig. 9, which contains the nucleon direct and crossed pole terms plus the delta direct and crossed terms. Hence there are 16 terms implicit in Fig. 8(b).

The s -wave $\pi N \rightarrow \pi N$ coupling is given by [28]

$$-i\delta\tilde{H} = -i4\pi\delta_{m_s m'_s} \left[\frac{2\lambda_1}{\mu} \delta_{m_i m'_i} \delta_{\lambda\lambda'} + i\epsilon_{\alpha\lambda\lambda'} \frac{\lambda_2}{\mu^2} (q^0 + q'^0) \langle m'_i | \tau^\alpha | m_i \rangle \right], \quad (15)$$

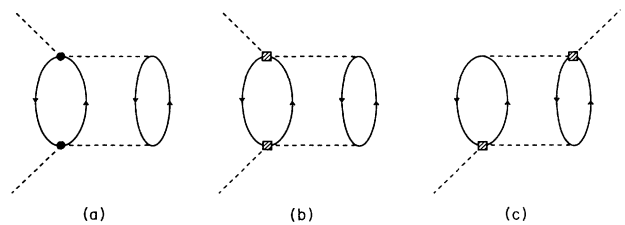


FIG. 8. Mechanisms for pion absorption: (a) s wave; (b) and (c) p wave. The solid circle indicates the s -wave πN amplitude, while the square represents the p -wave πN amplitude.

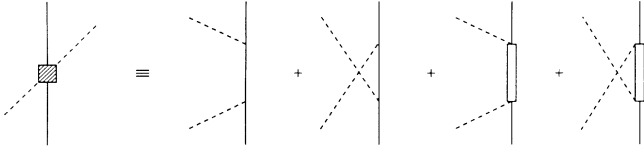


FIG. 9. Detail of the diagrams used in the model of Fig. 8 to represent the πN p -wave amplitude.

with λ_1 the isoscalar amplitude, λ_2 the isovector amplitude, and λ, λ' the pion isospin indices in Cartesian base. Since λ_1 is much smaller than λ_2 , we neglect it in our study. Then, for practical purposes, what matters in the isospin counting are the following isospin coefficients:

$$\begin{aligned} & 1 \text{ for } \langle \pi^+ p | \pi^+ p \rangle, \quad -1 \text{ for } \langle \pi^- p | \pi^- p \rangle, \\ & 1 \text{ for } \langle \pi^- n | \pi^- n \rangle, \quad -1 \text{ for } \langle \pi^+ n | \pi^+ n \rangle, \\ & \sqrt{2} \text{ for } \langle \pi^0 n | \pi^- p \rangle, \quad -\sqrt{2} \text{ for } \langle \pi^+ n | \pi^0 p \rangle, \end{aligned} \quad (16)$$

together with those for the πNN p -wave coupling discussed in the former section. Thus we can look at the basic diagram of Fig. 10 and compare the weight of the $\pi^+ nn \rightarrow \pi^- pp$ amplitude to the one of the $\pi^- NN \rightarrow \pi^- NN$, with $NN = pp$ or pn , which contribute to pion absorption. We can use only this direct diagram because the exchange diagrams in nuclear matter vanish in the limit $\lambda_1 = 0$ [28]. The counting is straightforward, and the result is

$$\begin{aligned} t^{(SA)} &= \int d^3x \phi_i^*(\mathbf{x}) \phi_j'(\mathbf{x}) e^{i(\mathbf{k}-\mathbf{k}')\cdot\mathbf{x}} \\ &\quad \times 4(4\pi) \left[1 + \frac{\varepsilon}{2} \right] B_0 \phi_i(\mathbf{x}) \phi_j(\mathbf{x}), \end{aligned} \quad (17)$$

with $\varepsilon = \omega/M$ and B_0 the absorption coefficient calculated in [28] such that the s -wave absorption pion self-energy ($2\omega V_{\text{opt}}$) is given by

$$\Pi^{(SA)} = -4\pi \left[1 + \frac{\varepsilon}{2} \right] B_0 \rho^2. \quad (18)$$

The values obtained in [28] for the B_0 parameter, which we use here, are

$$B_0 = [0.032 + i0.040] \mu^{-4}. \quad (19)$$

The counting is done here assuming only particle excitation to the right of the diagram of Fig. 10, while in [28] a large fraction of the real part came from Δ excitation. The counting done is thus correct for the imaginary part of $t^{(SA)}$ and only approximate for the real part.

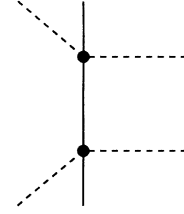


FIG. 10. Open diagram for s -wave absorption or absorption contribution to DCX.

One word of caution must be said about the procedure followed in the isospin counting. Indeed, selection rules appear when antisymmetry is properly considered; for instance, absorption from a $L=0, T=1$ initial pair is forbidden if $\lambda_1=0$ [33,34]. These selection rules are automatically implemented in our approach in nuclear matter as far as λ_1 is neglected, since the exchange terms vanish in this limit as indicated previously [28]. Yet, in finite nuclei, Eq. (17) gives a finite result even if $L=0$ in the initial state. Hence it is obviously incorrect in this case. The contradiction appears because in nuclear matter, where our counting is done, many partial waves are present in the initial state. Thus Eq. (17) can be a fair approximation in finite nuclei only when several partial waves are present in the nucleon-pair wave function. In ^{18}O there are many partial waves and in ^{14}C up to $L=2$. Therefore we expect the approximation of Eq. 17 to be rather good for the first case and just fair for ^{14}C .

Effects from the antisymmetry on the s -wave rescattering absorption of Fig. 10 were discussed in detail and considered in [28] where B_0 was calculated.

With respect to the diagrams in the p -wave absorption of Fig. 8(b) and 8(c), it was shown in [16] that there are cancellations and only some terms survive. We will follow the same notation for the terms as in [16] and write them in terms of the Δ excitation diagram of Fig. 3, which is still the dominant individual term for absorption, although it contributes only about one-third of the total absorption potential. We will refer to this diagram as $d1$. We depict the surviving diagrams in Fig. 11, and in Table I we give the relative weight of these diagrams at the pion threshold, both for pion absorption or absorption in double charge exchange. One can see in the table that in this latter case, although the individual terms are pretty large, there are also quite large cancellations between them, and the Δ excitation term accounts now for more than half of the strength. Although, the terms sum up to 1.85 times the amplitude of Eq. (11), but now $\hat{\Sigma}_\Delta$ is different from the resonance region. We then have

$$\begin{aligned} t^{(PA)} &= D \frac{4}{3} \frac{4}{9} \left[\frac{f^*}{\mu} \right]^2 \mathbf{k} \cdot \mathbf{k}' \frac{M^2}{\bar{s}} \int d^3x \phi_i^*(\mathbf{x}) \phi_j^*(\mathbf{x}) e^{i(\mathbf{k}-\mathbf{k}')\cdot\mathbf{x}} \phi_i^*(\mathbf{x}) \phi_j^*(\mathbf{x}) \left[\frac{1}{\sqrt{\bar{s}} - M_\Delta + i(\bar{\Gamma}/2) - \Sigma_\Delta} \right]^2 \\ &\quad \times \left\{ \frac{\text{Re} \hat{\Sigma}_\Delta}{\rho_0} + i \text{Im} \hat{\Sigma}_\Delta \frac{1}{\alpha \rho(\mathbf{r})} \arctan \left[\frac{\alpha \rho(\mathbf{r})}{\rho_0} \right] \right\}, \end{aligned} \quad (20)$$

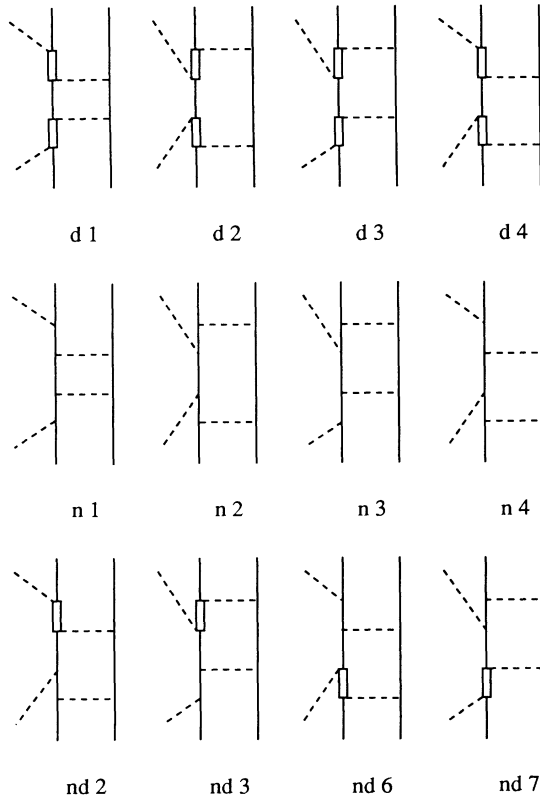


FIG. 11. Open diagrams for the p -wave absorption or absorption contribution to DCX. The nomenclature of the diagrams corresponds to the one in [16].

with

$$\text{Re}\hat{\Sigma}_{\Delta} = -53 \text{ MeV} + 0.11T_{\pi} \text{ MeV}, \quad 0 < T_{\pi} < 50 \text{ MeV},$$

$$\text{Im}\hat{\Sigma}_{\Delta} = -38.3 \left[1 - 0.85 \frac{T_{\pi}}{\mu} + 0.54 \frac{T_{\pi}^2}{\mu^2} \right] \text{ MeV}, \quad (21)$$

$$\alpha = 2.72 - 4.07 \frac{T_{\pi}}{\mu} + 3.07 \frac{T_{\pi}^2}{\mu^2},$$

$$D = 1.85 - 0.1 \frac{T_{\pi}}{\mu} - 1.33 \left[\frac{T_{\pi}}{\mu} \right]^2.$$

TABLE I. Contribution of the different terms of Fig. 11 to the absorption potential or the absorption DCX term. The term $d1$ accounts for the contribution of Eq. (4) to the pion self-energy, while the term $dx1$ corresponds to the contribution of Eq. (11) to the DCX amplitude.

Term	Pion absorption	DCX absorption
$d1$	$d1$	$dx1$
$d2$	$0.09d1$	$-3 \times 0.09dx1$
$d3+d4$	$0.07d1$	$3 \times 0.07dx1$
$n1$	$0.76d1$	$-4 \times 0.76dx1$
$n2$	$0.76d1$	0
$n3+n4$	$-0.17d1$	$-6 \times (-0.17)dx1$
$nd2+nd7$	$1.56d1$	$\frac{3}{4} \times 1.56dx1$
$nd3+nd6$	$-0.47dx1$	$-\frac{15}{4} \times (-0.47)dx1$
Total	$3.60d1$	$1.85dx1$

The term with arctan in Eq. (20) accounts for polarization effects when the ph excitation in Fig. 2(b) is iterated to all orders. For the conventional mechanism at low energies, we take the amplitude of the work of [7].

IV. RESULTS AND DISCUSSION

In the resonance region, we have taken into account the distortion of the pion waves by using Glauber theory as in [6]. For low energies we have not considered any distortion of the pion waves. The implementation of the distortion usually leads to an enhancement of the cross section by about a factor 2 with respect to the plane-wave results [29]. The wave functions used are as in [6,7] for ^{18}O and ^{14}C , respectively.

In Fig. 12 we can see the results of the differential cross section for the $^{18}\text{O}(\pi^+, \pi^-)^{18}\text{Ne}$ reaction at $T_{\pi} = 164$ MeV. The strength of the absorption mechanism is smaller than that of the conventional mechanism. We can also observe that the shapes of the two distributions are rather similar. At small angles the interference of the two amplitudes leads to a small reduction of the results of the conventional mechanism. However, around the region of the minimum, there is a stronger interference, which leads to a shift of the cross section at lower angles, from 34.5° to 30.5° . However, as one can see in the figure, the shift is not enough to move the minimum down to about 20° where there is the experimental minimum.

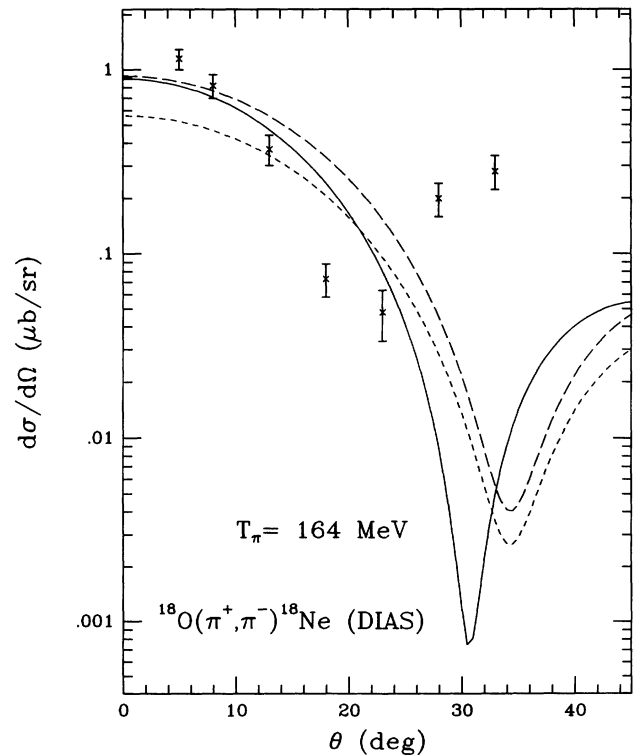


FIG. 12. Differential DCX cross section for $^{18}\text{O}(\pi^+, \pi^-)^{18}\text{Ne}$ (DIAS) at $T_{\pi} = 164$ MeV; long-dashed line, sequential mechanism; short-dashed line, absorption mechanism; solid line, sum of the two. Experimental data from [5].

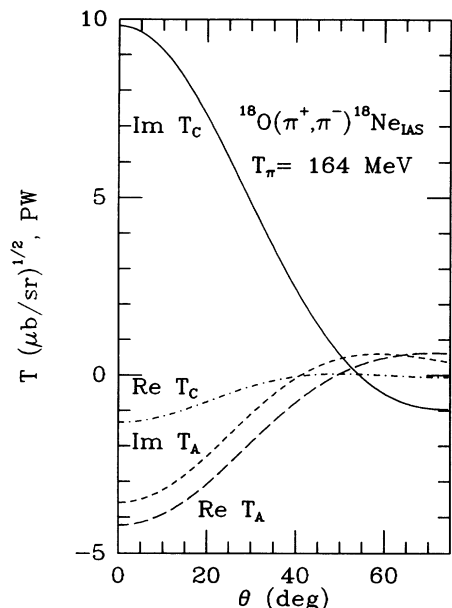


FIG. 13. Amplitudes for conventional and absorption contributions to DCX in ^{18}O at 164 MeV, calculated without distortion: solid line, imaginary part of conventional mechanism; dot-dashed line, real part of conventional mechanism; short-dashed line, imaginary part of absorption mechanism; long-dashed line, real part of absorption mechanism.

According to our arguments in Sec. II, we should have expected a stronger interference of these amplitudes. In practice, however, we ended up with a weak one. The reason is the strong effect of distortion in this process. This can be seen in Figs. 13 and 14 where we show the amplitudes corresponding to conventional and absorption mechanisms with and without distortion. Without distortion, the amplitude of the conventional mechanism is almost imaginary and the absorption mechanism has a

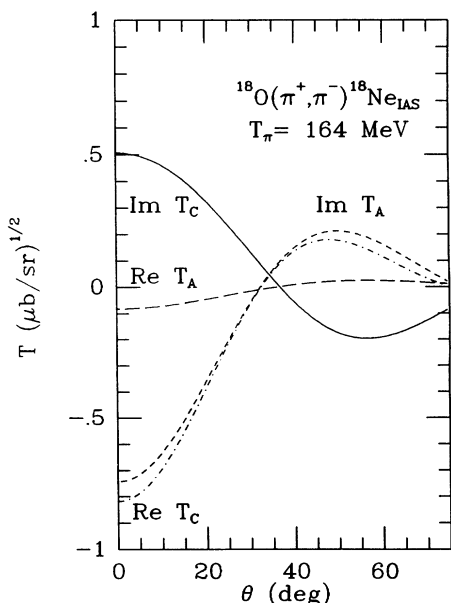


FIG. 14. Same as Fig. 13 with distortion.

sizable imaginary part, as was expected. However, when distortion is included, it affects differently both the size and phase of the two amplitudes in such a way that interference does not modify strongly the cross section. This also tells us that we must accept some intrinsic uncertainties in our results since small variations in the wave functions or details in the distortion mechanisms can easily change the final results. We believe these uncertainties to be not smaller than a factor of 2 in the cross section at forward angles and bigger at large angles. Our results should be thus taken as indicative of the relative effects of one mechanism to the other, and the size of the shift must be also taken at a qualitative level. However, we can say that it is unlikely that the new mechanism produces larger shifts than observed in our calculations, since small changes in the value of g' , or the Δ self-energy, do not lead to appreciable changes in the size of the shift.

In Fig. 15 we show the results for $^{14}\text{C}(\pi^+, \pi^-)$ DIAS at $T_\pi = 50$ MeV. The conventional mechanism has been taken from [7], and we have added to it coherently the amplitude obtained here. The results are without distortion as we indicated. From Fig. 15 it follows that at low energies the absorption mechanism is an important piece of the DCX reaction mechanism. At large angles the conventional and absorption mechanisms are comparable. At small angles the absorption mechanism is smaller than the conventional since there is strong destructive interference in the absorption amplitude between the s - and p -wave parts around 50 MeV. The interference between

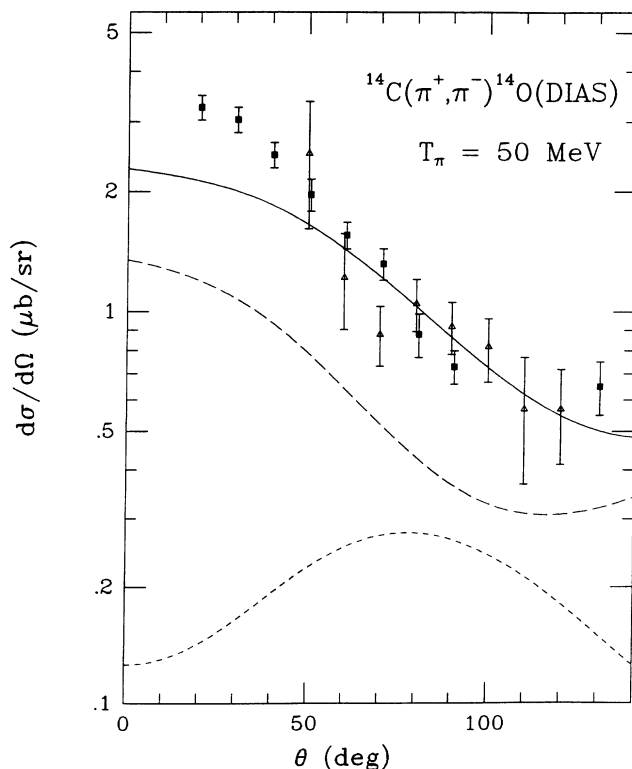


FIG. 15. Differential cross section for $^{14}\text{C}(\pi^+, \pi^-)$ DIAS at $T_\pi = 50$ MeV: long-dashed line, sequential mechanism; short-dashed line, absorption mechanism; solid line, sum of the two. Experimental data from [3].

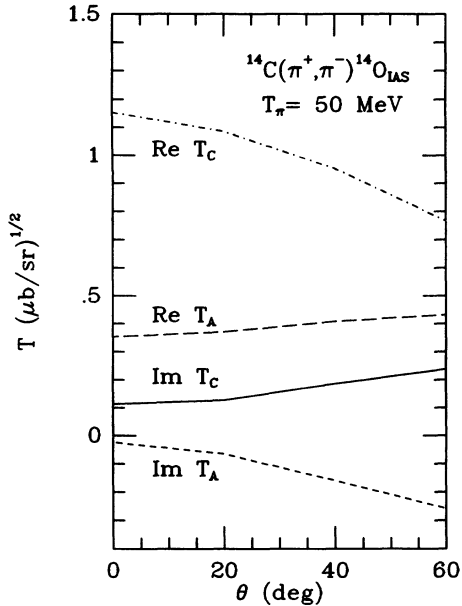


FIG. 16. DCX amplitudes for conventional and absorption contributions to DCX at 50 MeV in ^{14}C . The meaning of the lines is the same as in Fig. 14.

the conventional and absorption mechanisms is constructive, as shown in Fig. 16, and enhances appreciably the results with respect to those of the conventional mechanism. The final results are closer to the experimental ones, but one should have in mind that there is no distortion in the results and that other mechanisms such as exchange currents also lead to modifications of these results [30].

We only want to draw qualitative conclusions since we believe that also at low energies, as in the resonance region, one has intrinsic uncertainties stemming from an incomplete control of the information needed for the exchange currents, plus the large sensitivity of the results to the quantities involved in the process, which, even if small, also have uncertainties. The real parts used in the absorption mechanism also suffer from larger uncertainties than the imaginary parts [16,28]. The effect of the absorption mechanism, like the one of the exchange currents, decreases with increasing A because of the fact that the processes involve the contribution of short-range

forces [31]. We can see this qualitatively by evaluating the effects of the exchange currents in ^{16}O , which are smaller than in ^{14}C , although the structure of the wave function is also partly responsible.

V. CONCLUSIONS

Within certain reasonable approximations, consistent with the qualitative nature of our analysis, we have evaluated the contribution of the absorption mechanism to DCX, both at low energies and at resonance. At low energies the absorption mechanism interferes constructively with the sequential mechanism around $T_\pi = 50$ MeV, and in the case of $^{14}\text{C}(\pi^+, \pi^-)$ DIAS it increases the cross section by about 60% at small angles and around a factor of 2 at larger angles.

Around resonance, the effects are globally very small, but the approximately destructive interference leads to a small shift of the first diffraction minimum in the $^{18}\text{O}(\pi^+, \pi^-)$ DIAS at $T_\pi = 164$ MeV, which is not sufficient to explain the experimental data.

As has occurred before with other mechanisms studied, the sequential mechanism stands as the most important mechanism of the reaction, at least for the DIAS transitions, but the corrections can lead to appreciable changes in the results. The study carried out here indicates that, at least in light nuclei, the effect of the absorption mechanism has to be included if one attempts an accurate and realistic evaluation of DCX. However, we should also stress that, at present, there are still intrinsic uncertainties in the input which result in uncertainties in the cross section of DCX of the order of factors of 2 or more.

ACKNOWLEDGMENTS

E. Oset would like to thank the hospitality of the Joint Institute for Nuclear Research in Dubna where the work was started, H. Sarafian and M. Khankhasayev of the Department of Theoretical Physics of the University of Valencia, and the Institute for Nuclear Theory of Seattle where the work was concluded. J. Nieves wishes to acknowledge the financial support from Ministerio de Educación y Ciencia. This work has been partly supported by the CICYT Contract No. AEN 90-0049. The calculations have been done in the Centro Informático de la Universidad de Valencia.

[1] *Proceedings of the International Workshop of DCX*, Los Alamos, 1989, edited by W. R. Gibbs, and J. J. Leitch (World Scientific, Singapore, 1990).
 [2] *Proceedings of the International Workshop on Pions in Nuclei*, Peniscola, 1991, edited by E. Oset, M. J. Vicente-Vacas, and C. García-Recio (World Scientific, Singapore, 1992).
 [3] I. Navon *et al.*, Phys. Rev. Lett. **52**, 105 (1984); A. Altman, *ibid.* **55**, 1273 (1985); M. J. Leitch *et al.*, *ibid.* **54**, 1492 (1985); M. J. Leitch *et al.*, Phys. Rev. C **39**, 2356 (1989).
 [4] F. Irom *et al.*, Phys. Rev. Lett. **55**, 1862 (1985); J. U. Ullman *et al.*, Phys. Rev. C **33**, 2092 (1986).
 [5] S. J. Green *et al.*, Phys. Lett. **88B**, 62 (1979); Kamal K. Seth *et al.*, Phys. Rev. Lett. **43**, 1574 (1979); **45**, 147

(1980); S. J. Green *et al.*, Phys. Rev. C **25**, 927 (1982).
 [6] E. Oset, M. J. Vicente-Vacas, M. B. Johnson, D. Strottman, H. T. Fortune, and R. Gilman, Nucl. Phys. **A488**, 514 (1988).
 [7] E. R. Siciliano, M. B. Johnson, and H. Sarafian, Ann. Phys. (N.Y.) **203**, 1 (1990).
 [8] P. Hoodbhoy, R. J. Freedman, G. A. Miller, and E. M. Henley, Phys. Rev. C **27**, 277 (1983).
 [9] D. S. Koltun and M. S. Singham, Phys. Rev. C **41**, 2266 (1990).
 [10] E. Oset, M. J. Vicente-Vacas, and Ma Wei-Hsing, Nucl. Phys. **A408**, 461 (1983); E. Oset, D. Strottman, M. J. Vicente-Vacas, and Ma Wei-Hsing, Phys. Rev. C **34**, 2349 (1986).
 [11] M. F. Jiang and D. S. Koltun, Phys. Rev. C **42**, 2662

- (1990).
- [12] P. Hoodbhoy, R. A. Freeman, G. A. Miller, and E. M. Henley, *Phys. Rev. C* **27**, 277 (1983).
- [13] K. Stricker, J. A. Carr, and H. MacManus, *Phys. Rev. C* **19**, 929 (1979); **22**, 2043 (1980); J. A. Carr and H. MacManus, *ibid.* **27**, 952 (1981).
- [14] M. Khankhasayev, *Nucl. Phys.* **A505**, 717 (1989).
- [15] A. W. Thomas and R. M. Landau, *Phys. Rep.* **58**, 121 (1980).
- [16] J. Nieves, E. Oset, and C. García-Recio, *Nucl. Phys.* (to be published).
- [17] C. García-Recio, E. Oset, L. L. Salcedo, D. Strottman, and M. J. López, *Nucl. Phys.* **A526**, 685 (1991).
- [18] H. J. Weyer, *Phys. Rep.* **195**, 295 (1990).
- [19] L. C. Liu, in *Proceedings of LAMPF Workshop on pion double charge exchange*, Los Alamos, 1985, Los Alamos Report No. LA-10550-C, 1985, p. 109.
- [20] R. Gilman *et al.*, *Nucl. Phys.* **A432**, 610 (1985).
- [21] M. B. Johnson, E. R. Siciliano, H. Toki, and A. Wirzba, *Phys. Rev. Lett.* **52**, 593 (1984).
- [22] E. Oset and L. L. Salcedo, *Nucl. Phys.* **A468**, 631 (1987).
- [23] Y. Horikawa, M. Thies, and F. Lenz, *Nucl. Phys.* **A345**, 386 (1980).
- [24] L. L. Salcedo, E. Oset, M. J. Vicente, and C. García-Recio, *Nucl. Phys.* **A484**, 557 (1988).
- [25] J. Speth, E. Werner, and W. Wild, *Phys. Rep. C* **33**, 127 (1977).
- [26] F. Mandl and G. Shaw, *Quantum Field Theory* (Wiley, New York, 1988).
- [27] J. D. Bjorken and S. D. Drell, *Relativistic Quantum Fields* (McGraw-Hill, New York, 1965).
- [28] C. García-Recio, E. Oset, and L. L. Salcedo, *Phys. Rev. C* **37**, 194 (1988).
- [29] T. Karapiperis and M. Kobayashi, *Ann. Phys. (N.Y.)* **177**, 1 (1981).
- [30] M. B. Johnson, E. Oset, H. Sarafian, M. Siciliano, and M. J. Vicente-Vacas, *Phys. Rev. C* **44**, 2480 (1991).
- [31] E. Oset, M. J. Vicente-Vacas, and D. Strottman, in *Proceedings of the 2nd International Workshop on Double Charge Exchange*, Los Alamos, 1989, edited by W. R. Gibbs and J. J. Leitch (World Scientific, Singapore, 1990), p. 351.
- [32] M. J. Vicente-Vacas and E. Hernandez, in *Proceedings of the International Workshop on Pions in Nuclei* [2], p. 471; C. García Recio, J. Nieves, and E. Oset, in *ibid.*, p. 320.
- [33] T. Ericson and W. Weise, *Pions in Nuclei* (Oxford University Press, New York, 1988), p. 267.
- [34] D. S. Koltun and A. Reitan, *Phys. Rev.* **141**, 1413 (1966).